Theoretical and Applied Fracture Mechanics 67–68 (2013) 38–45

Contents lists available at ScienceDirect

Theoretical and Applied Fracture Mechanics

journal homepage: www.elsevier.com/locate/tafmec

Mode I stress intensity factor for cracked thin-walled composite beams

Franco E. Dotti *, Víctor H. Cortínez [1], Florencia Reguera [1]

Centro de Investigación en Mecánica Teórica y Aplicada, Facultad Regional Bahía Blanca, Universidad Tecnológica Nacional, 11 de Abril 461, B8000LMI Bahía Blanca, Argentina
Consejo Nacional de Investigaciones Científicas y Técnicas, Av. Rivadavia 1917, C1033AAJ Ciudad Autónoma de Buenos Aires, Argentina

ARTICLE INFO

Article history:
Available online 22 October 2013

Keywords:
G^* integral
Thin-walled beam
Fiber reinforced composite
Stress intensity factor
Fracture mechanics

ABSTRACT

In this paper, we present an analytical method to determine the mode I stress intensity factor for thin-walled beams made of laminated composites. The technique relies on the concept of crack surface widening energy release rate, which is expressed in terms of the G^* integral and thin-walled beam theory. In the vicinity of the crack tip, a solution of the G^* integral is obtained employing stress and displacement fields derived for materials with general orthotropy. The effect of warping is taken into account. This is a common feature in thin-walled beams which cannot be neglected, especially when flexural–torsional loads are present.

The model shows a good agreement with finite element results. It is shown that, although the approaches developed for isotropic materials may be useful in the treatment of orthotropic problems, they may not yield good results for some typical lamination sequences.

© 2013 Elsevier Ltd. All rights reserved.

1. Introduction

Slender members made of composite materials are widely employed in modern engineering structures. As a result, the study of fracture mechanics in such structural components has become a topic of recognized importance. A significant parameter of fracture mechanics is the stress intensity factor (SIF), which plays an important role in the evaluation of the structural integrity. In complex structures, this parameter is usually determined by means of finite element calculations. This strategy has proven to give good results [1], but in some cases it can be expensive due to the need of large models or highly refined meshes. It is known that, in the context of Structural Health Monitoring, calculations must be performed in real time. Consequently, it is desirable to obtain simple formulas in order to save computation time.

Most fracture mechanics approaches for linear elastic materials are based on stress and displacement fields obtained for isotropic materials [2–5]. These techniques can be applied directly in a limited range of orthotropic problems [6]. But if a complex anisotropy is present or more accuracy is required, a method developed specifically for composites must be considered. For solid section beams, some authors studied the fracture mechanics in composites with orthotropic lamination [7–9]. The proposed techniques rely on the expression of the energy release rate proposed by Nikpur and Dimarogonas [10], using the SIFs given by Bao and coworkers [11,12]. All these latter approaches used the crack tip results derived by Sih et al. [6].

Besides the complexity addressed by the use of non-isotropic materials, the treatment of thin-walled beams involves additional complications due to the presence of cross-sectional warping and flexural–torsional couplings [13–15]. Although some approaches for isotropic structural profiles have been presented [4,16–18], to the authors' knowledge, only one regards the warping effect [19].

In this article we present a simple formula to determine the mode I SIF for cracked thin-walled beams, made of fiber reinforced composites. The technique is based on the G^* integral concept [5,20] and thin-walled beam theory, in conjunction with conservation law and classical lamination theory [15,21,22]. G^* integral solution is obtained regarding stress and displacement fields for materials with general orthotropy [6]. The influence of cross-sectional warping is taken into account by considering the energetic contribution of the bimomental force.

2. Crack tip stress and displacement fields for an orthotropic lamina

Laminate composites consist of an arrangement of orthotropic laminas as the one sketched in Fig. 1. Each lamina verifies the existence of two planes of constructive symmetry which are mutually perpendicular and simultaneously normal to a third plane. The angle Φ indicates the orientation of the fibers with respect to the laminate coordinate system.

* Corresponding author at: Centro de Investigación en Mecánica Teórica y Aplicada, Facultad Regional Bahía Blanca, Universidad Tecnológica Nacional, 11 de Abril 461, B8000LMI Bahía Blanca, Argentina. Tel.: +54 291 4555220; fax: +54 291 4555311.

E-mail address: fdotti@frbb.utn.edu.ar (F.E. Dotti).

[1] Tel.: +54 291 4555220; fax: +54 291 4555311.

0167-8442/$ - see front matter © 2013 Elsevier Ltd. All rights reserved.
http://dx.doi.org/10.1016/j.tafmec.2013.10.002

Nomenclature

a_{ij}	elastic constants of a composite lamina
a	crack depth (also semi-major axis of the elliptic crack)
$\tilde{a}$	variable crack depth
A	cross-sectional area
$\overline{A}_{11}$	laminate plate stiffness coefficient
b	dimension of a flange
B	bimomental beam force (also point B, origin of the system B: x, s, n)
$\overline{B}_{11}$	laminate plate stiffness coefficient
c	semi-minor axis of the elliptic crack
C	center of gravity of the uncracked cross section
C_w	warping constant
C_θ	constant obtained from solving the G^* integral in a quarter of circle
$\overline{D}_{11}$	laminate plate stiffness coefficient
f_i	stress field functions
g_i	displacement field functions
G^*	crack mouth widening energy release rate
h	dimension of the web
I_y, I_z	second moments of area
I_{yz}	product moment of area
$I_{y\omega}$, $I_{z\omega}$	product of warping
$\mathbf{J}$	constitutive matrix of the beam
J_{ij}	components of the constitutive matrix
K_I	Mode I stress intensity factor
l	distance in n direction from C to a point in the cross-section middle line
L	length of the beam
n	coordinate normal to the cross-section middle line
N	axial beam force
M_y, M_z	bending moments
p_j	complex number
q_j	complex number
$\mathbf{Q}$	vector of generalized forces
r	radial coordinate
s	circumferential coordinate
S	cross-sectional perimeter
S_y, S_z	first moments of area
S_ω	first moment of warping
t	beam thickness
$\mathbf{T}$	stress vector
T_x, T_s	elements of the stress vector
u	axial displacement of the uncracked beam centroid
u_x	axial displacement of any point of the beam
u_s	circumferential displacement of any point of the beam
$\mathbf{u}$	displacement vector
U	strain energy
U_0	strain energy density
x, y, z	Cartesian coordinates
x_i	Cartesian coordinates of the intrinsic system of a lamina
Y, Z	coordinates of a point located in the middle line of the cross-section
Γ	integration path
γ_{ij}	angular strain in a composite lamina
ε_{ij}	normal strain in a composite lamina
$\mathbf{\Delta}$	vector of generalized strains
$\boldsymbol{\eta}$	unit outward normal vector
η_x, η_s	components of the unit outward normal vector
θ	angular coordinate
θ_x	warping variable
θ_y, θ_z	bending twists
λ	auxiliary integration variable
μ_i	complex number
ν	Poisson's ratio
ξ	crack location (axial coordinate)
Π	total potential energy
σ_{ij}	stresses in a composite lamina
ω_p	primary warping function
Φ	orientation angle of the fibers
$(\bullet)_0$	subscript associated to the uncracked cross-section
$(\bullet)_{\tilde{a}}$	subscript associated to the cracked cross-section (with x integration variable)
$(\bullet)_\lambda$	subscript associated to the cracked cross-section (with λ integration variable)

Considering a plain stress condition, the constitutive law for such orthotropic lamina can be expressed as

$$\begin{Bmatrix} \varepsilon_{xx} \\ \varepsilon_{ss} \\ \gamma_{xs} \end{Bmatrix} = \begin{bmatrix} a_{11} & a_{12} & a_{16} \\ a_{12} & a_{22} & a_{26} \\ a_{16} & a_{26} & a_{66} \end{bmatrix} \begin{Bmatrix} \sigma_{xx} \\ \sigma_{ss} \\ \sigma_{xs} \end{Bmatrix}, \tag{1}$$

where a_{ij} (i = 1, 2, 6) are constants which depend on the elastic properties of the composite and the orientation angle Φ of the lamina [15].

For mode I loading, Sih et al. [6] derived the stress and displacement fields near the crack tip in a rectilinearly anisotropic body as

$$\sigma_{xx} = (2\pi r)^{-\frac{1}{2}} K_I f_1(\theta), \tag{2}$$

$$\sigma_{ss} = (2\pi r)^{-\frac{1}{2}} K_I f_2(\theta), \tag{3}$$

$$\sigma_{xs} = (2\pi r)^{-\frac{1}{2}} K_I f_3(\theta), \tag{4}$$

and

$$u_x = (2r)^{\frac{1}{2}} \pi^{-\frac{1}{2}} K_I g_1(\theta), \tag{5}$$

$$u_s = (2r)^{\frac{1}{2}} \pi^{-\frac{1}{2}} K_I g_2(\theta), \tag{6}$$

respectively. These fields are expressed in terms of a polar coordinate system of variables r and θ, whose origin is located at the crack tip, as in Fig. 2. The functions $f_i(\theta)$ and $g_i(\theta)$, involving material properties, are given by

$$f_1(\theta) = \mathrm{Re}\left[\frac{1}{\mu_1 - \mu_2}\left(\frac{\mu_1}{\sqrt{\cos\theta + \mu_2 \sin\theta}} - \frac{\mu_2}{\sqrt{\cos\theta + \mu_1 \sin\theta}}\right)\right], \tag{7}$$

$$f_2(\theta) = \mathrm{Re}\left[\frac{\mu_1\mu_2}{\mu_1 - \mu_2}\left(\frac{\mu_2}{\sqrt{\cos\theta + \mu_2 \sin\theta}} - \frac{\mu_1}{\sqrt{\cos\theta + \mu_1 \sin\theta}}\right)\right], \tag{8}$$

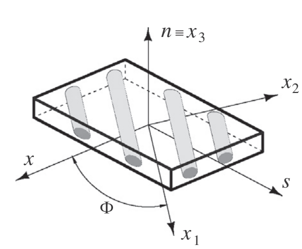

Fig. 1. Composite lamina with general orthotropy. Relation among the laminate coordinate system (B: x, s, n) and the intrinsic system of the lamina (B: x_1, x_2, x_3).

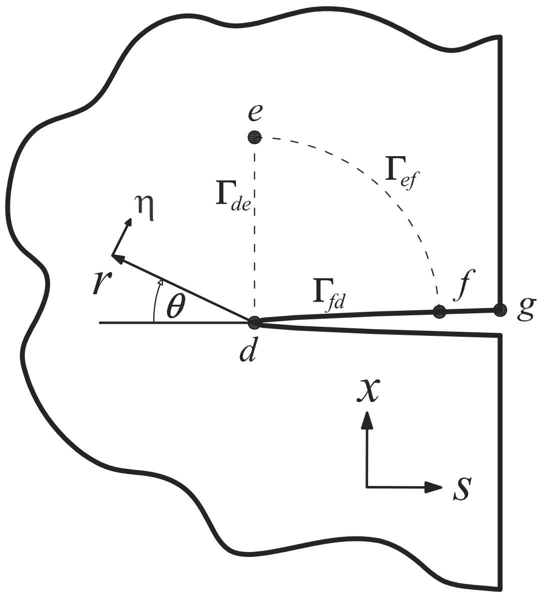

Fig. 2. Two-dimensional simplification of a three-dimensional edge-crack.

$$f_3(\theta) = \mathrm{Re}\left[\frac{\mu_1\mu_2}{\mu_1-\mu_2}\left(\frac{1}{\sqrt{\cos\theta+\mu_1\sin\theta}}-\frac{1}{\sqrt{\cos\theta+\mu_2\sin\theta}}\right)\right], \quad (9)$$

$$g_1(\theta) = \mathrm{Re}\left[\frac{1}{\mu_1-\mu_2}\left(\mu_1 q_2\sqrt{\cos\theta+\mu_2\sin\theta}-\mu_2 q_1\sqrt{\cos\theta+\mu_1\sin\theta}\right)\right], \quad (10)$$

$$g_2(\theta) = \mathrm{Re}\left[\frac{1}{\mu_1-\mu_2}\left(\mu_1 p_2\sqrt{\cos\theta+\mu_2\sin\theta}-\mu_2 p_1\sqrt{\cos\theta+\mu_1\sin\theta}\right)\right], \quad (11)$$

where $p_j = a_{22}\mu_j^2 + a_{12} - a_{26}\mu_j$ and $q_j = a_{12}\mu_j + a_{11}/\mu_j - a_{16}$. In order to find the complex numbers μ_j, the characteristic equation

$$a_{22}\mu^4 - 2a_{26}\mu^3 + (2a_{12}+a_{66})\mu^2 - 2a_{16}\mu + a_{11} = 0, \quad (12)$$

must be solved for each lamina.

3. G^* integral and mode I SIF for an orthotropic lamina

Let the crack sketched in Fig. 2 be a two-dimensional simplification of a three-dimensional edge-crack in a composite lamina. From the conservation law, the two-dimensional G^* integral can be defined per unit thickness as [5,20]

$$G^* = \int_\Gamma \left(U_0\eta_x - \mathbf{T}\frac{\partial \mathbf{u}}{\partial x}\right) d\Gamma, \quad (13)$$

where U_0 is the strain energy density, $\boldsymbol{\eta} = \{\eta_x, \eta_s\}$ is the unit outward normal and $\mathbf{T} = \{T_x, T_s\}$ is the stress vector applied on the outer side of the path Γ. The vector $\mathbf{u} = \{u, v\}$ contains the displacements from the Sih–Paris–Irwin field [6], given in (5), (6). When G^* is solved for the path Γ_{dfg}, it represents the energy release rate due to the moving crack boundary dfg in the x direction. As the crack mouth opens, G^* can be regarded as the crack mouth widening energy release rate [5].

Being the paths Γ_{de} and Γ_{ef} a straight line and a quarter of circle respectively, Eq. (13) can be solved to yield

$$\int_{\Gamma_{de}} \left(U_0\eta_x - \mathbf{T}\frac{\partial \mathbf{u}}{\partial x}\right) d\Gamma = \frac{K_I^2 \log r}{4\pi}[f_1(\pi/2) + g_1(\pi/2) + f_3(\pi/2)(g_2(\pi/2) + 2g_1'(\pi/2)) + 2f_2(\pi/2)g_2'(\pi/2)] = 0, \quad (14)$$

and

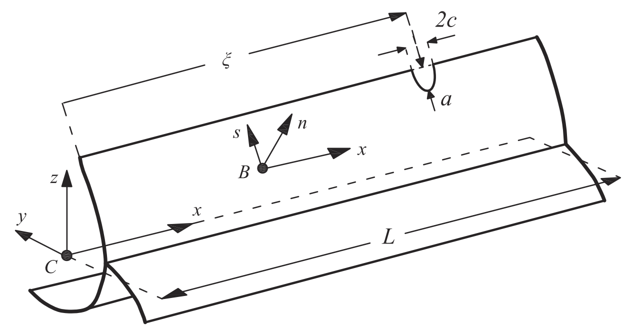

Fig. 3. Generic thin-walled beam with a crack regarded as an elliptical hole ($c \to 0$).

$$\int_{\Gamma_{ef}} \left(U_0\eta_x - \mathbf{T}\frac{\partial \mathbf{u}}{\partial x}\right) d\Gamma = \frac{K_I^2 C_\theta}{4\pi}, \quad (15)$$

where K_I is the mode I SIF and C_θ is a constant inherent to the lamina and given by

$$C_\theta = \int_{\pi/2}^{\pi} \{f_1(\theta)\sin\theta(g_1(\theta)\sin\theta + 2g_1'(\theta)\cos\theta) + f_2(\theta)[g_2(\theta)\cos\theta\sin\theta + g_2'(\theta)(3+\cos 2\theta)] + f_3(\theta)[g_1(\theta)\cos\theta\sin\theta + g_2(\theta)\sin^2\theta + g_1'(\theta)(3+\cos 2\theta) + g_2'(\theta)\sin 2\theta]\}\, d\theta. \quad (16)$$

The integral in Eq. (16) can be easily solved numerically.

From the conservation law, Eq. (13) vanishes for all closed paths, therefore solving it for $\Gamma_{defd} = \Gamma_{de} + \Gamma_{ef} - \Gamma_{df}$ must produce $\oint_{\Gamma_{defd}}(U_0\eta_x - T\partial x)d\Gamma = 0$. Employing Eqs. (14) and (15), it follows that

$$\oint_{\Gamma_{defd}} \left(U_0\eta_x - \mathbf{T}\frac{\partial \mathbf{u}}{\partial x}\right) d\Gamma = \int_{\Gamma_{def}} \left(U_0\eta_x - \mathbf{T}\frac{\partial \mathbf{u}}{\partial x}\right) d\Gamma - \int_{\Gamma_{df}} \left(U_0\eta_x - \mathbf{T}\frac{\partial \mathbf{u}}{\partial x}\right) d\Gamma = \frac{K_I^2 C_\theta}{4\pi} - \int_{\Gamma_{df}} \left(U_0\eta_x - \mathbf{T}\frac{\partial \mathbf{u}}{\partial x}\right) d\Gamma = 0. \quad (17)$$

Now, considering Eq. (17), G^* can be expressed as

$$G^* = \int_{\Gamma_{dfg}} \left(U_0\eta_x - \mathbf{T}\frac{\partial \mathbf{u}}{\partial x}\right) d\Gamma = \frac{K_I^2 C_\theta}{4\pi} + \int_{\Gamma_{fg}} U_0\, d\Gamma. \quad (18)$$

Eq. (18) must be interpreted as the energy release rate per unit moving of boundary Γ_{dfg} in x direction. The material properties and the orientation of the lamina are condensed in C_θ, within the functions $f_i(\theta)$ and $g_i(\theta)$.

4. Energy release rate for cracked thin-walled composite beams

4.1. A cracked thin-walled composite beam

Fig. 3 shows a sketch of a generic thin-walled beam with an edge crack. The points of the beam are referred to a Cartesian coordinate system (C: x, y, z), which origin C is located at the centroid of the uncracked cross-section. A circumferential coordinate s and a normal coordinate n are also defined in the middle line of the cross-section. A point on this middle line has coordinates Y and Z. The system (B: x, s, n) is consistent with the laminate system defined in Fig 1.The crack is located at $x = \xi$ and regarded as an elliptical hole under the condition of $c \to 0$ [20]. Hence, the crack depth is variable with x as

$$\tilde{a}(x) = a\sqrt{1 - \frac{(x-\xi)^2}{c^2}}. \quad (19)$$

4.2. Constitutive law

The constitutive equation associated to a thin-walled composite beam can be written as [15]

$$\mathbf{Q} = \mathbf{J}\boldsymbol{\Delta}, \quad (20)$$

where $\mathbf{Q}$ is the vector of generalized beam forces, $\mathbf{J}$ the constitutive matrix and $\boldsymbol{\Delta}$ the vector of generalized strains. Since only the application of mode I loads are considered, the energy contributions of shear and torque are small and can be neglected. Hence, the expressions of $\mathbf{Q}$ and $\boldsymbol{\Delta}$ can be expressed are

$$\mathbf{Q} = \{N, M_y, M_z, B\}^T, \quad (21)$$

$$\boldsymbol{\Delta} = \left\{\frac{\partial u}{\partial x}, -\frac{\partial \theta_y}{\partial x}, -\frac{\partial \theta_z}{\partial x}, -\frac{\partial \theta_x}{\partial x}\right\}^T. \quad (22)$$

The following generalized beam forces have been defined in Eq. (21): N as the axial force, M_y and M_z as the bending moments and B as the bimoment. Since mode I loading is considered, the couplings associated to shear and torsion are neglected. The generalized strains in vector $\boldsymbol{\Delta}$ are defined in terms of the generalized displacements: u as the axial displacement, θ_y and θ_z as the bending rotations and θ_x as the warping variable. The constitutive matrix $\mathbf{J}$, defined in Eq. (20), is a symmetric matrix containing the cross-sectional magnitudes and the laminate properties. The components of $\mathbf{J}$ are given by

$$\begin{aligned}
&J_{11} = E^*A, \quad J_{12} = E^*S_y + \overline{B}_{11}\int_S \tfrac{dY}{ds}\,ds, \quad J_{13} = E^*S_z - \overline{B}_{11}\int_S \tfrac{dZ}{ds}\,ds,\\
&J_{14} = E^*S_\omega - \overline{B}_{11}\int_S l\,ds, \quad J_{22} = E^*I_y + 2\overline{B}_{11}\int_S Z\tfrac{dY}{ds}\,ds + \overline{D}_{11}\int_S \left(\tfrac{dY}{ds}\right)^2 ds,\\
&J_{23} = E^*I_{yz} - \overline{B}_{11}\int_S \left(Z\tfrac{dZ}{ds} - Y\tfrac{dY}{ds}\right) ds - \overline{D}_{11}\int_S \tfrac{dY}{ds}\tfrac{dZ}{ds}\,ds,\\
&J_{24} = E^*I_{y\omega} + \overline{B}_{11}\int_S \left(\tfrac{dY}{ds}\omega_p - lZ\right) ds - \overline{D}_{11}\int_S l\tfrac{dY}{ds}\,ds,\\
&J_{33} = E^*I_z - 2\overline{B}_{11}\int_S Y\tfrac{dZ}{ds}\,ds + \overline{D}_{11}\int_S \left(\tfrac{dZ}{ds}\right)^2 ds,\\
&J_{34} = E^*I_{z\omega} - \overline{B}_{11}\int_S \left(\tfrac{dZ}{ds}\omega_p + lY\right) ds + \overline{D}_{11}\int_S l\tfrac{dZ}{ds}\,ds,\\
&J_{44} = E^*C_w - 2\overline{B}_{11}\int_S l\omega_p\,ds + \overline{D}_{11}\int_S l^2\,ds,
\end{aligned} \quad (23)$$

where $l = Y\,dY/ds + Z\,dZ/ds$ and

$$\begin{aligned}
&A = t\int_S ds, \quad S_y = t\int_S Z\,ds, \quad S_z = t\int_S Y\,ds, \quad S_\omega = t\int_S \omega_p\,ds,\\
&I_y = t\int_S Z^2\,ds, \quad I_z = t\int_S Y^2\,ds, \quad I_{yz} = t\int_S YZ\,ds,\\
&I_{y\omega} = t\int_S Z\omega_p\,ds, \quad I_{z\omega} = t\int_S Y\omega_p\,ds, \quad C_w = t\int_S \omega_p^2\,ds.
\end{aligned} \quad (24)$$

In Eqs. (23) and (24), S denotes the contour perimeter of the cross-section, t is the wall thickness, ω_p is the primary warping function [15], $E^* = \overline{A}_{11}/t$ and $\overline{A}_{11}, \overline{B}_{11}, \overline{D}_{11}$ are laminate plate stiffness coefficients [15,21,22]. No change in the warping function is considered due to the presence of the crack. Eqs. (23) and (24) are valid at any cross section of the beam. If it is an intact cross-section, perimeter S takes the constant value S_0. If the elliptical crack as defined in (19) is present, S becomes $S_{\tilde{a}}$, which depends on $\tilde{a}$.

4.3. Energy release rate

The strain energy related to the generic beam in Fig. 3 can be expressed as

$$U = \frac{1}{2}\left[\int_0^{\xi-c} \mathbf{Q}^T\mathbf{J}_0^{-1}\mathbf{Q}\,dx + \int_{\xi-c}^{\xi+c} \mathbf{Q}^T\mathbf{J}_{\tilde{a}}^{-1}\mathbf{Q}\,dx + \int_{\xi+c}^{L} \mathbf{Q}^T\mathbf{J}_0^{-1}\mathbf{Q}\,dx\right], \quad (25)$$

where $\mathbf{J}_{\tilde{a}}$ and $\mathbf{J}_0$ are the constitutive matrices associated to the cracked and uncracked cross-section, respectively. $\mathbf{J}_{\tilde{a}}$ depend on x through expression (19).

Now, neglecting the small alterations generated in the beam forces by the presence of the crack, the expression (25) can be reformulated as

$$U = \frac{1}{2}\left[\int_0^{\xi-c} \mathbf{Q}^T\mathbf{J}_0^{-1}\mathbf{Q}\,dx + c\mathbf{Q}^T\Big|_{x=\xi}\int_{-1}^{1}\mathbf{J}_\lambda^{-1}\,d\lambda\mathbf{Q}|_{x=\xi} + \int_{\xi+c}^{L} \mathbf{Q}^T\mathbf{J}_0^{-1}\mathbf{Q}\,dx\right], \quad (26)$$

where an additional integration variable has been defined as $\lambda = (x-\xi)/c$.

From Clapeyron's theorem, the work of external loads is $V = 2\,U$. The potential energy is given by $\Pi = U - V$, therefore $\Pi = -U$. Then the crack surface widening energy release rate can be expressed as

$$G^* = \lim_{c\to 0}\frac{\partial U}{\partial c} = \frac{1}{2}\frac{\partial}{\partial c}\left(\int_0^{\xi-c} \mathbf{Q}^T\mathbf{J}_0^{-1}\mathbf{Q}\,dx + \int_{\xi+c}^{L} \mathbf{Q}^T\mathbf{J}_0^{-1}\mathbf{Q}\,dx\right) + \mathbf{Q}^T\Big|_{x=\xi}\int_0^1 \mathbf{J}_\lambda^{-1}\,d\lambda\mathbf{Q}|_{x=\xi} \quad (27)$$

This expression can be rearranged by applying the fundamental theorem of calculus to give

$$G^* = \mathbf{Q}^T\Big|_{x=\xi}\left(\int_0^1 \mathbf{J}_\lambda^{-1}\,d\lambda - \mathbf{J}_0^{-1}\right)\mathbf{Q}|_{x=\xi}. \quad (28)$$

5. Mode I SIF

Eqs. (18) and (28) are obtained by different paths, but they both represent the crack mouth widening energy release rate G^*. Following the ideas of Xie et al. [5,16,18], these expressions can be equated to obtain

$$\frac{K_I^2 C_\theta}{4\pi} + \int_{\Gamma_{fg}} U_0\,d\Gamma = \frac{1}{t}\left[\mathbf{Q}^T\Big|_{x=\xi}\left(\int_0^1 \mathbf{J}_\lambda^{-1}\,d\lambda - \mathbf{J}_0^{-1}\right)\mathbf{Q}|_{x=\xi}\right]. \quad (29)$$

Now, due to free action of crack surface, the contribution of the integral on Γ_{fg} is a small quantity which can be disregarded. Thus, the mode I SIF is given by

$$K_I = \sqrt{\frac{4\pi}{tC_\theta}\left[\mathbf{Q}^T\Big|_{x=\xi}\left(\int_0^1 \mathbf{J}_\lambda^{-1}\,d\lambda - \mathbf{J}_0^{-1}\right)\mathbf{Q}|_{x=\xi}\right]}. \quad (30)$$

Eq. (30) shows that the SIF depends on crack depth a, generalized beam forces in cracked cross-sectional area $\mathbf{Q}|_{x=\xi}$, material properties, laminate properties and orientation of the lamina through C_θ, beam thickness t and properties of cracked and uncracked cross-section condensed in $\mathbf{J}_{\tilde{a}}$ and $\mathbf{J}_0$, respectively. Expression (30) is generic and can be applied to edge-cracked thin-walled

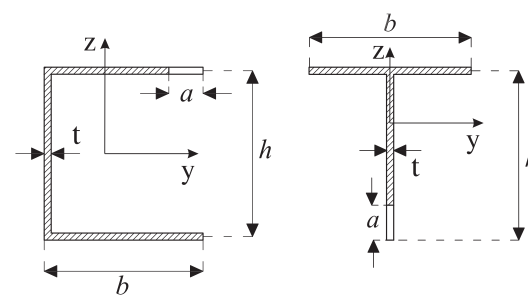

Fig. 4. Cross-sectional shapes used and its corresponding crack dispositions.

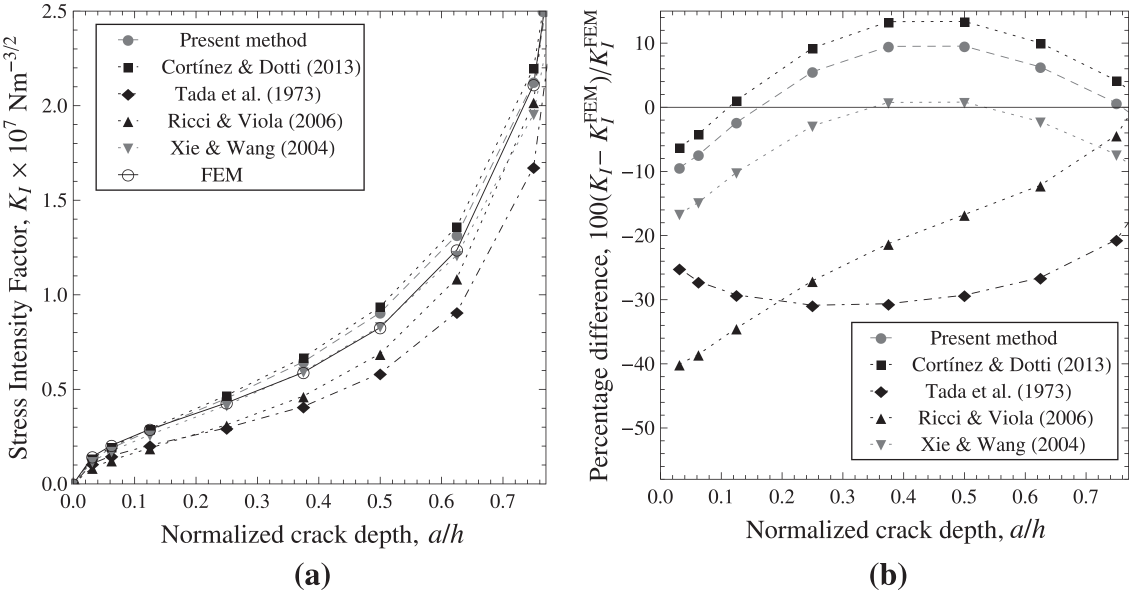

Fig. 5. (a) SIF for a cracked thin-walled T-beam under bending (M_y = 1 kN m, no warping). Laminate: $\{0\}_4$. (b) Percentage difference with respect to FEM results.

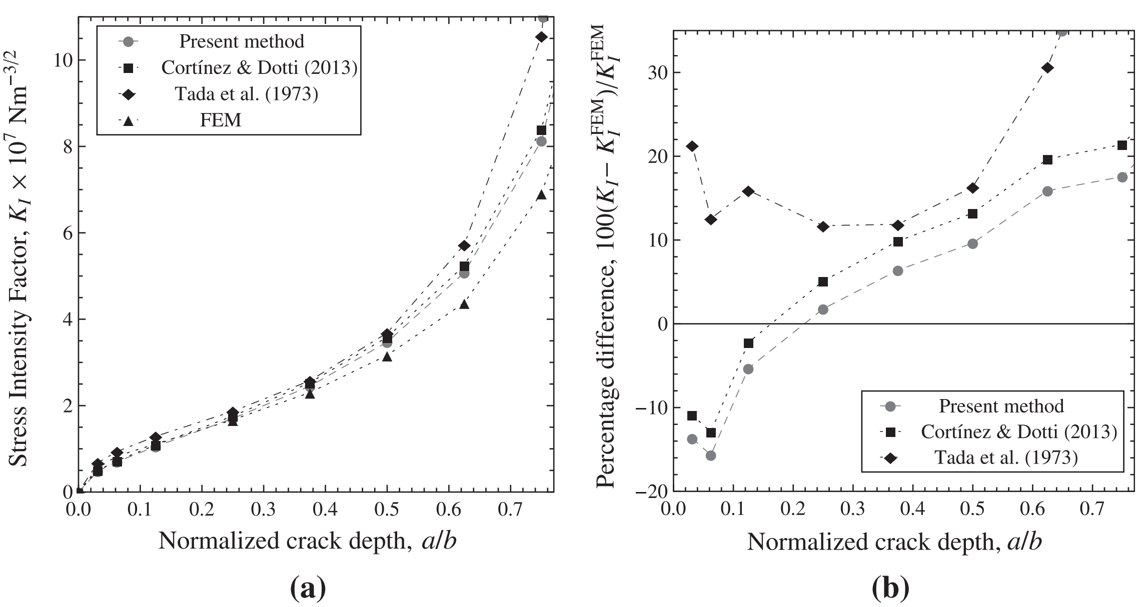

Fig. 6. (a) SIF for a cracked thin-walled U-beam under bending (M_z = 3 kN m, no warping). Laminate: $\{0\}_4$. (b) Percentage difference with respect to FEM results.

beams of any cross-section, made of fiber reinforced composite materials with any fiber orientation, for mode I loading.

6. Results and discussion

We present comparisons of the results obtained by Eq. (30) against the results by finite element method (FEM) and by other authors when available. In FEM analysis, we employed ABAQUS 6.7 package [23,24], meshing with 20-node quadratic brick elements (C3D20R). Quarter point singularity elements were assigned to the neighborhood of crack tip. Each mesh consisted of about 120000 elements.

The analyzed cross-sectional shapes are shown in Fig. 4: a U-profile with a crack at one of its flanges and a T-profile with a crack in the web. For both cases, the dimensions considered were h = 0.2 m, b = 0.1 m, t = 0.01 m and L = 2 m. Crack location was set to $\xi/L = 0.5$. Graphite–epoxy (AS4/3501) with different laminate schemes was considered in the calculations. Material properties are: E_1 = 1.44 GPa, E_2 = 9.65 GPa, ν_{12} = 0.3, G_{12} = 4.14 GPa, G_{23} = 3.45 GPa, ρ = 1389 kg/m^3.

In their seminal paper [6], Sih, Paris and Irwin noted that the classic approach for isotropic materials may be directly applied to orthotropic problems for individual examples. This scenario was represented by the example of Fig. 5, corresponding to a T-beam with a 0° lamination. Results from Eq. (30) were compared with FEM and results by other authors [16,4,19]. A rearrangement of classical K_I formulas [2] was included, by considering the cracked web as an independent plate with statically equivalent loading (indicated in figures as Tada et al.). Considering FEM results as reference, the method presented in this paper showed an acceptable performance for a wide range of crack depths, with errors in the order of 15% for moderate depths. The approach of

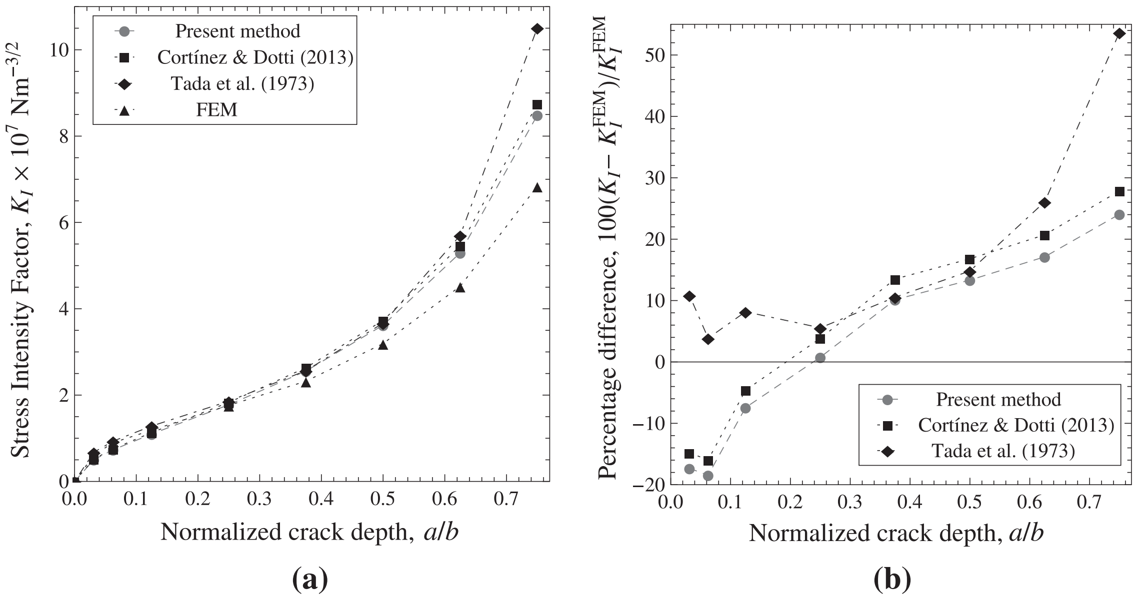

Fig. 7. (a) SIF for a cracked thin-walled U-beam under bending (M_z = 3 kN m, B = −2.30 N m^2). Laminate: $\{45/-45\}_s$. (b) Percentage difference with respect to FEM results.

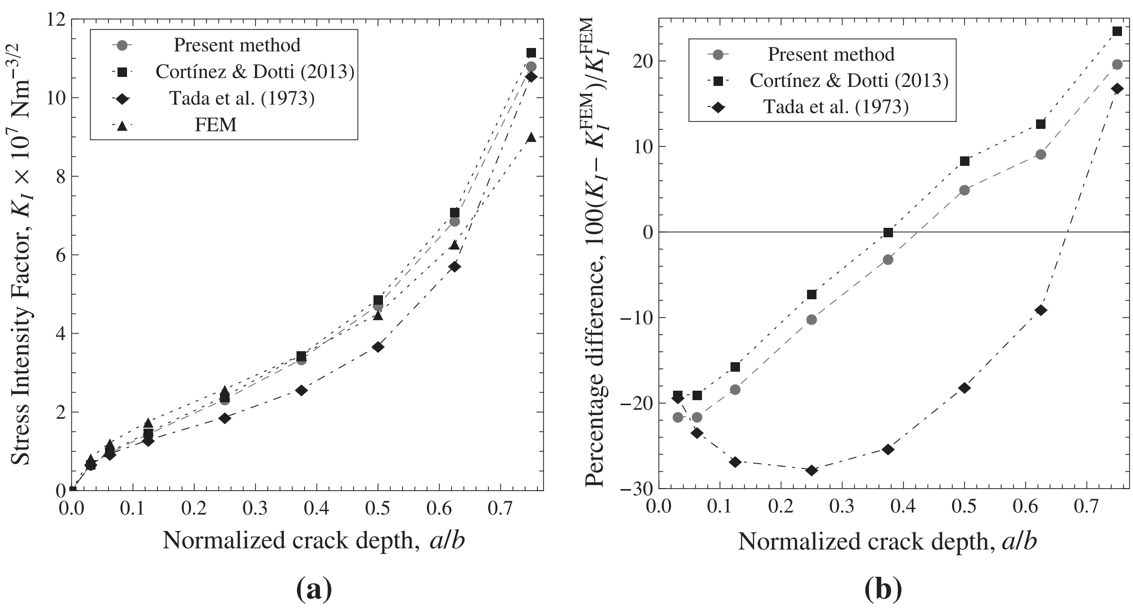

Fig. 8. (a) SIF for a cracked thin-walled U-beam under bending (M_z = 3 kN m, no warping). Laminate: $\{0/90\}_s$, curves corresponding to 0° laminas. (b) Percentage difference with respect to FEM results.

Cortínez and Dotti, developed for isotropic thin-walled beams [19], and Xie and Wang's formula for T-beams [16] gave also similar results, as can be expected since they all derive from G^* integral concept. Classical formula errors were in the order of 30% while Ricci and Viola's formula [4] failed to 40% difference for very small cracks. In any case, these results should not be considered as bad if one takes into account the simplicity of the aforementioned approaches.

For isotropic U-beams, some authors [4,16] presented SIF's formulas which consider the presence of two symmetrical cracks at the flanges. With the exception of method from Ref. [19], there are no approaches addressed in the literature for a U-beam having a single crack at one flange. Predictions become more difficult in the latter case since the crack introduces an asymmetry, which increases with depth, resulting in a strong three-dimensional behavior of the beam. The U-beam studied in the example of Fig. 6 had a 0° lamination. Present method showed acceptable agreement with FEM results, as well as the approach for isotropic thin-walled beams by Cortínez and Dotti [19]. While approaches from Refs. [4,16] are not applicable, adapted classical formula gave good results for small to moderate cracks.

Sih, Paris and Irwin claims were also satisfied for the case of a composite U-beam made with a symmetric and balanced laminate, as can be seen in the results of Fig. 7. Isotropic approaches give good results, and also similar results to the present approach.

A very common stacking sequence employed in composites is symmetric cross-ply lamination. For 0° and 90° laminas in a $\{0/90\}_s$ laminate, results are presented in Figs. 8 and 9, respectively.

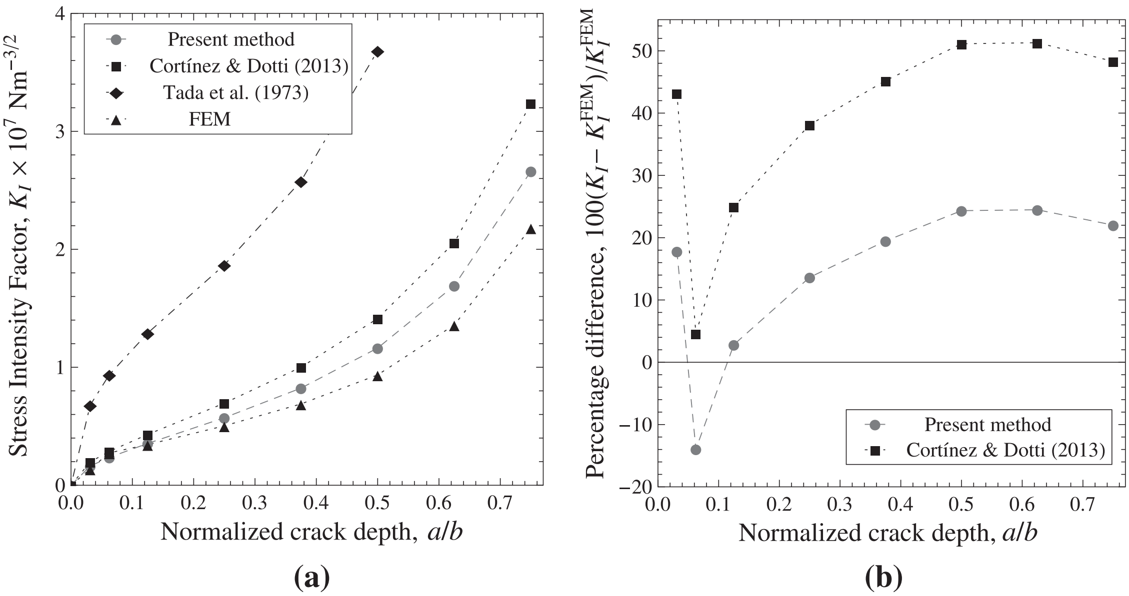

Fig. 9. (a) SIF for a cracked thin-walled U-beam under bending (M_z = 3 kN m, no warping). Laminate: $\{0/90\}_s$, curves corresponding to 90° laminas. (b) Percentage difference with respect to FEM results.

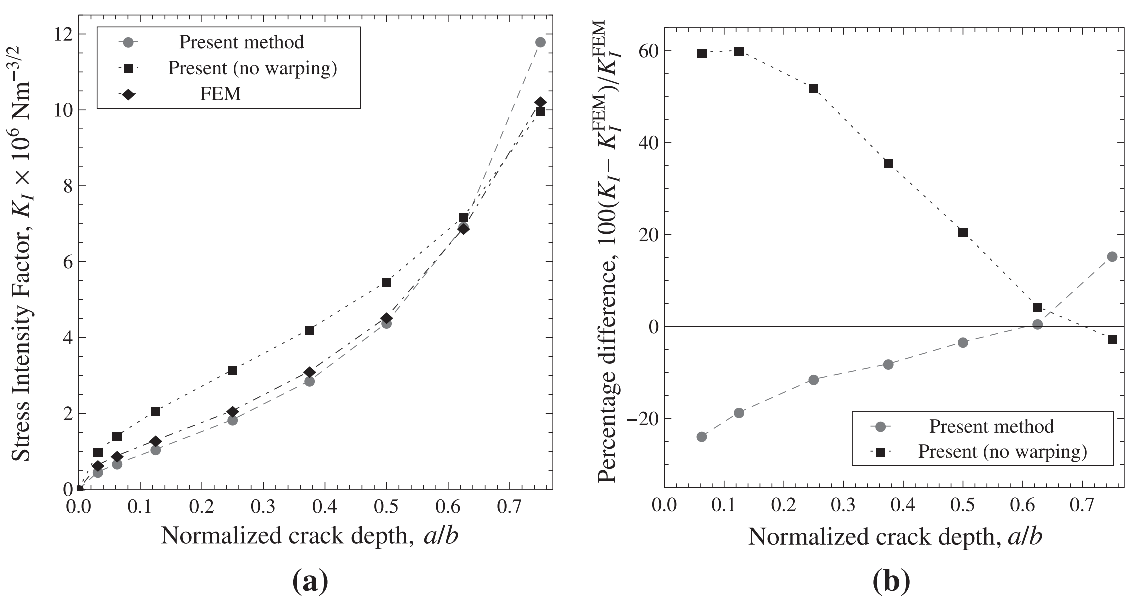

Fig. 10. (a) SIF for a cracked thin-walled U-beam under bending (M_y = 1 kN m, B = −62.44 N m^2; "no warping" implies considering B = 0). Laminate: $\{0/90\}_s$, curves corresponding to 0° laminas. (b) Percentage difference with respect to FEM results.

For this example, FEM calculations showed a SIF highly dependent on the angle of lamination. For moderate cracks, present approach yielded acceptable results for both, 0° and 90° laminas. Isotropic approaches worked well for 0° laminas but failed for 90° laminas, as can be seen in Fig. 9. Results from classical formula were the same for both laminas, since it do not consider the influence of material properties. Method from Ref. [19] gave a better approximation, but still failed up to 50% for some moderate cracks.

Also for symmetric cross-ply laminate, we present the results of Figs. 10 and 11. In this example, we considered a load which generates a very strong flexural–torsional coupling in order to quantify the influence of warping. Results of present method with and without the influence of bimomental force were compared against FEM results. It can be seen that the fact of neglecting the influence of cross-sectional warping leads to important errors in SIF prediction.

7. Conclusions

A new formula to determine the mode I SIF for cracked thin-walled composite beams is presented. It represents an extension to composite materials with respect to the method previously presented by the authors for isotropic materials [19].

The accuracy of the formula was tested against results by finite element method (FEM) and other authors when available, for some common lamination sequences. Considering FEM results as reference, the method presented in this paper showed an acceptable performance for practical engineering applications (errors in the order of 15% for moderate crack depths). For very small or very large cracks, errors in estimating the SIF are inevitable for simplified approaches, which are derived from a one-dimensional standpoint.

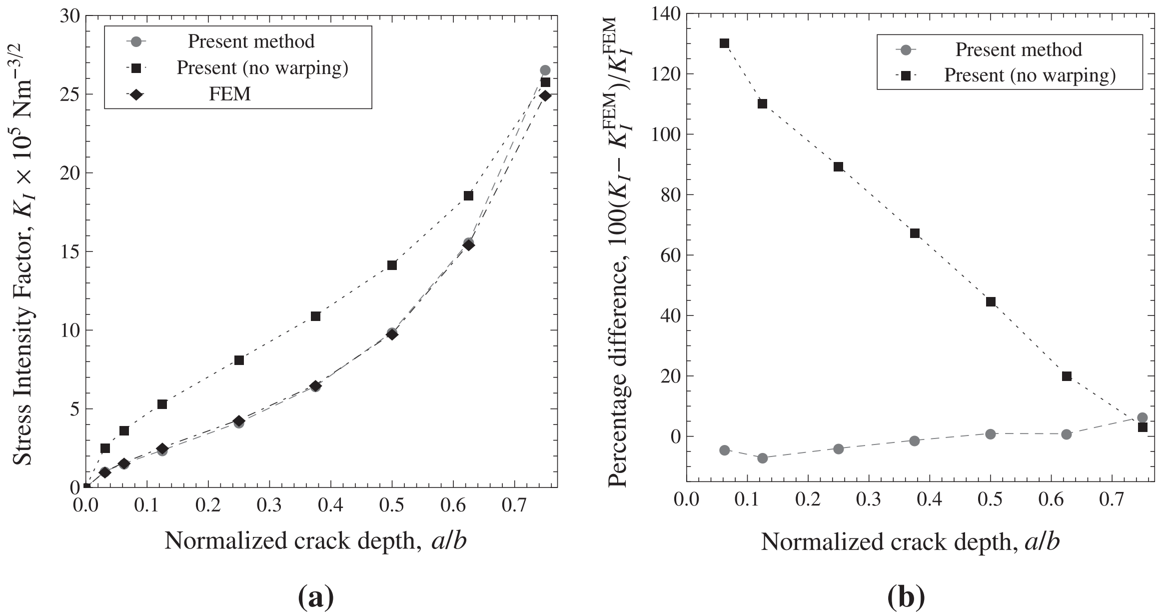

Fig. 11. (a) SIF for a cracked thin-walled U-beam under bending (M_y = 1 kN m, B = −62.44 N m^2; "no warping" implies considering B = 0). Laminate: $\{0/90\}_s$, curves corresponding to 90° laminas. (b) Percentage difference with respect to FEM results.

For orthotropic laminates, although in general terms the present method yields better results, it is shown that approaches derived for isotropic materials can be used without major problems. This also seems to be applicable to some balanced symmetric laminates. But for a common lamination sequence as symmetric cross-ply, methods developed for isotropic materials can produce wrong results, requiring the use of models derived specifically for composites, as the one presented in this article.

This method takes into account a very common feature in thin-walled beams: the warping effect. This is performed by considering the energetic contribution of the bimomental force. It is shown that neglecting the influence of warping leads to errors in predicting the SIF, especially if strong flexural–torsional couplings are present.

The proposed formula represents a contribution in health monitoring and failure analysis of slender structures.

Acknowledgements

The authors would like to thank the support of Secretaría de Ciencia y Tecnología of Universidad Tecnológica Nacional and CONICET. The present article is part of the doctoral thesis by Franco Dotti, under the direction of Víctor Cortínez and Marcelo Piovan, at the Department of Engineering of Universidad Nacional del Sur.

References

[1] S. Courtin, C. Gardin, G. Bézine, H. Ben Hadj Hamouda, Advantages of the J-integral approach for calculating stress intensity factors when using the commercial finite element software ABAQUS, Eng. Fract. Mech. 72 (2005) 2174–2185.
[2] H. Tada, P.C. Paris, G.R. Irwin, Stress Analysis of Cracks Handbook, Del Research Corporation, Hellertown, 1973.
[3] L. Nobile, Mixed mode crack initiation and direction in beams with edge crack, Theor. Appl. Fract. Mech. 33 (2000) 107–116.
[4] P. Ricci, E. Viola, Stress intensity factors for cracked T-sections and dynamic behavior of T-beams, Eng. Fract. Mech. 73 (2006) 91–111.
[5] Y.J. Xie, H. Xu, P.N. Li, Crack mouth energy-release rate and its application, Theor. Appl. Fract. Mech. 29 (3) (1998) 195–203.
[6] G.C. Sih, P.C. Paris, G.R. Irwin, On cracks in rectilinearly anisotropic bodies, Int. J. Fract. Mech. 1 (1965) 189–203.
[7] O. Song, T.W. Ha, L. Librescu, Dynamics of anisotropic composite cantilevers weakened by multiple transverse open cracks, Eng. Fract. Mech. 70 (2003) 105–123.
[8] M. Kisa, Free vibration analysis of a cantilever composite beam with multiple cracks, Compos. Sci. Technol. 64 (2004) 1391–1402.
[9] K. Wang, D.J. Inman, C.R. Farrar, Modeling and analysis of a cracked composite cantilever beam vibrating in coupled bending and torsion, J. Sound Vib. 284 (2005) 23–49.
[10] K. Nikpur, A. Dimarogonas, Local compliance of composite cracked bodies, Compos. Sci. Technol. 32 (1998) 209–223.
[11] Z. Suo, G. Bao, B. Fan, T.C. Wang, Orthotropy rescaling and implications for fracture in composites, Int. J. Solids Struct. 28 (2) (1991) 235–248.
[12] G. Bao, S. Ho, Z. Sou, B. Fan, The role of material orthotropy in fracture specimens for composites, Int. J. Solids Struct. 29 (1992) 1105–1116.
[13] V.Z. Vlasov, Thin Walled Elastic Beams, Israel Program for Scientific Translation, Jerusalem, 1961.
[14] A. Gjelsvik, Theory of Thin Walled Beams, John Wiley & Sons, New York, 1981.
[15] V.H. Cortínez, M.T. Piovan, Vibration and buckling of composite thin-walled beams with shear deformability, J. Sound Vib. 258 (4) (2002) 701–723.
[16] Y.J. Xie, X.H. Wang, Application of G^* integral on cracked structural beams, J. Constr. Steel Res. 60 (2004) 1271–1290.
[17] E. Ghafoori, M. Motavalli, Analytical calculation of stress intensity factor of cracked steel I-beams with experimental analysis and 3D digital image correlation measurements, Eng. Fract. Mech. 78 (2011) 3226–3242.
[18] Y.J. Xie, X.H. Wang, Y.C. Lin, Stress intensity factors for cracked rectangular cross-section thin-walled tubes, Eng. Fract. Mech. 71 (2004) 1501–1513.
[19] V.H. Cortínez, F.E. Dotti, Mode I stress intensity factor for cracked thin-walled open beams, Eng. Fract. Mech. 110 (2013) 249–257.
[20] Y.J. Xie, P.N. Li, H. Xu, On K_I estimates of cracked pipes using an elliptical hole model and elementary beam strength theory of cracked beams, Eng. Fract. Mech. 59 (3) (1998) 399–402.
[21] E.J. Barbero, Introduction to Composite Material Design, Taylor and Francis Group, Ann Arbor, 1998.
[22] L.P. Kollár, G.S. Springer, Mechanics of Composite Structures, Cambridge University Press, New York, 2003.
[23] ABAQUS Analysis Manual v6.7. Dassault Systèmes, 2007.
[24] ABAQUS Theory Manual v6.7. Dassault Systèmes, 2007.